International Journal of
Physical and Chemical Sciences
https://www.ioro.org/ijpcs

Atmospheric Reactions of HFE-7100 with HO_2 and NH_2 radicals: Kinetics Mechanism and Atmospheric implications

Narendra Pramanik[1], Devaprasad Dev[*2], Nand Kishor Gour[3], Bhupesh Kumar Mishra[*4]

[1]*Department of Chemistry, Himalayan University, Jollang-791109, Arunachal Pradesh, India*

[2]*Department of Chemical Sciences, Tezpur University, Tezpur, Napaam, Assam – 784 028, India*

[3]*Department of Chemistry, Dera Natung Government College, Itanagar, 791113, Arunachal Pradesh, India*

Abstract

In recent pasts, HFE-7100 finds its industrial applications like cleaning electronic equipment, secondary refrigerant and carrier fluids for lubricant. Detailed theoretical investigations have been carried out on the mechanism, kinetics and thermochemistry of the gas-phase reactions between $CF_3CF_2CF_2CF_2OCH_3$ (HFE-7100) and HO_2 and NH_2 radicals using DFT-based M06-2X/6-311++G(d,p) level of theory. Two important H abstraction channels have been identified and one transition state has been located for each reaction channel. The pre-reactive and post-reactive complexes are validated at entrance and exit channels, respectively. The potential energy surface of the HFE-7100 with HO_2 and NH_2 radicals has been investigated using DFT method. The rate constants of the two reactions are computed over the temperature range of 250–450 K for the first time. Our results suggest that hydrogen abstraction by NH_2 radical is likely the dominant route for the atmospheric oxidation of HFE-7100 under reaction conditions.

Keywords: Segregated HFE, M06-2X, DFT, Rate constant, Amino radical

1. Introduction

It is well known fact that hydrofluoroethers (HFEs) are designed and widely recommended as a third generation replacement for chlorofluorocarbons (CFCs), hydrofluorocarbon (HFC) and hydrochlorofluorocarbon (HCFC) in industrial applications [1-2]. $C_4F_9OCH_3$ (HFE-7100), $C_4F_9OC_2H_5$ (HFE-7200) and $C_7F_{15}OC_2H_5$ (HFE-7500) are classified as Segregated hydrofluoroethers i.e. ethers with fluorocarbon on one side of the oxygen atom and hydrocarbon on the other. $C_4F_9OCH_3$ (methoxynonafluorobutane) is commercially available as trade name of HFE-7100 and finds its industrial applications like cleaning electronic equipment, secondary refrigerant and carrier fluids for lubricant. Due to its lower global warming potential HFE-7100 has been proposed to replace FC-72 (C_6F_{14}) [3]. They are also being used as fluorous solvents for the chemical processing of organic electronic materials [4]. By employing relative rate technique Wallington *et al.* [5] reported a rate constant of 1.2×10^{-14} cm^3 $molecule^{-1}$ s^{-1} at 295 K for reaction of HFE-7100 with OH radicals. Subsequently, Cavalli *et al.*[6] performed another experimental study and reported a significantly lower rate constant value of $(7.2 \pm 1.6) \times10^{-15}$ cm^3 $molecule^{-1}$ s^{-1} at 295±3 K. Bravo *et al.*[7] experimentally studied the temperature dependence of n- $C_4F_9OCH_3$ + OH reaction over the temperature range of 288-368 K and reported the value of (1.49 ± 0.13) 10^{-14} cm^3 $molecule^{-1}$ s^{-1}. Wallington *et al.*[5] and Aranda *et al.*[8] experimentally measured studied Cl-initated hydrogen abstraction of HFE-7100 and reported a rate constant

International Journal of Physical and Chemical Sciences (IJPCS)
Volume 1 | Issue 1 | 2026 | Article ID: 9285-9098-3894 | https://doi.org/10.64823/ijpcs.2601006
IORO Publications · Texas, USA · www.ioro.org

values as k(Cl + n-$C_4F_9OCH_3$) = (9.7±1.4) 10^{-13} and k(Cl + n-$C_4F_9OCH_3$) = (1.43 ± 0.28) 10^{-13} cm^3 $molecule^{-1}$ s^{-1} at 298 K, respectively. Recently, Mishra *et al*. [9] reported the rate constant for the atmospheric reaction of n-$C_4F_9OCH_3$ with OH and Cl radicals and also explored the fate of alkoxy radicals using DFT method.

To the best of our knowledge, the mechanism and kinetics of the reaction between HFE-7100 and HO_2 & NH_2 radicals have not yet been investigated both theoretically and experimentally. Due to the lack of rate constant, the reaction of HFE-7100 with HO_2 & NH_2 radicals should be researched fully and carefully. Therefore, the PES characterizing the HFE-7100 +HO_2/ NH_2 reaction has been theoretically figured out in the present work. In present work, we have studied the mechanism and kinetics of H-abstraction reaction from HFE-7100 with HO_2 and NH_2 radicals using DFT methods. Our calculations suggest that only one reaction channel is feasible for n-$C_4F_9OCH_3$ + HO_2/NH_2 reactions as given below.

n- $C_4F_9OCH_3$ + HO_2 → n- $C_4F_9OCH_2$ + H_2O_2 (1)

n- $C_4F_9OCH_3$ + NH_2 → n- $C_4F_9OCH_2$ + NH_3 (2)

2. Computational methods

All electronic structure computations were carried out using the Gaussian 09 software package [10]. Density functional theory (DFT) calculations were performed employing the M06-2X hybrid functional [11] in conjunction with the 6-311++G(d,p) basis set. The M06-2X functional is well recognized for its reliable performance in predicting thermochemical properties and reaction kinetics and has demonstrated good agreement with experimental and theoretical results in numerous prior studies [12-17]. Harmonic vibrational frequency analyses were conducted at the same level of theory to characterize the nature of the optimized stationary points and to obtain zero-point energy corrections. These calculations confirmed that stable species correspond to true minima with no imaginary frequencies, whereas each transition state exhibits a single imaginary frequency associated with the reaction coordinate. Intrinsic reaction coordinate (IRC) calculations [18] were further performed to ensure that each transition state properly connects the relevant reactant and product minima. Using the optimized geometries obtained at the M06-2X/6-311++G(d,p) level, more accurate single-point energy calculations were subsequently carried out and the resulting energies were used to evaluate the relative energy differences (ΔE) among all stationary points.

3. Results and discussion

At the M06-2X/6-311++G(d,p) level, the calculated thermodynamic data for the species has been recorded in Table 1. The reaction enthalpies (Δ_rH°) and free energies (Δ_rG°) at 298 K for loss processes (12) are documented in Table 1. These thermodynamic functions were determined with thermal corrections to the energy at 298 K. The calculated $\Delta_rH°$ and $\Delta_rG°$ values at 298 K indicate that reaction channel 2 is more thermodynamically viable. Because $\Delta_rH^\circ_{298} < 0$, the results also show that reaction channel 2 is exothermic in nature.

The reaction channels (1 2) proceed with pre-reactive complexes (RC1 and RC2) in the entrance channel for while for the exit channel product complexes, referred as PC1 and PC2 were also obtained before the formation of final products. The electronic structure of the optimized geometry of the reactants, products, reaction complexes, product complexes and transition states obtained at the M06-2X/6-311++G(d,p) level are shown in Fig. 1. Hydrogen abstraction by HO_2 radical corresponding to reaction channel (1), visualization of the electronic structure of optimized geometry of TS1 revealed that the breaking CH (C2 H14) bond length is elongated from 1.090 to 1.370 Å along with shrinkage of CO bond from 1.437 to 1.395 Å. Similarly, for

transition state TS2 corresponding to reaction channel 2, the length of the breaking CH bond (C2 H14) is found to be elongated by 17.79% than the observed CH bond length in isolated HFE-7100 molecule whereas the CO (C2 O3) bond is shortened to 1.416 to 1.437 Å than the CO bond length in isolated HFE-7100 molecule. Table 2 presents the results of the harmonic vibrational frequency calculation at the M06-2X/6-311++G(d,p) level. Each transition state has one imaginary frequency due to its first order saddle point character, while the analysis of the harmonic vibrational frequency of minima including reactants, reactant complexes (RCs), product complexes (PCs), and products revealed no imaginary frequency (NIMAG=0). The C2–H14 and O19–H14 stretching modes are represented by the imaginary frequency of TS1 for reaction channel (1), which is 1792 cm^{1}. This also shows a considerable curvature in the potential energy surface (PES) surrounding the transition state. The imaginary frequency for transition state corresponding to the hydrogen abstraction by NH_2 radical is found to be 1849 cm^{1}, which corresponds to the stretching modes for hydrogen transfer reaction C2–H14 and N19–H14.

The representation of the normal-mode corresponding to the calculated imaginary frequencies shows a clear transition state geometry connecting reactants and products during transition. To further ascertain whether a transition state exists on the potential energy surface, the intrinsic reaction coordinate (IRC) calculation [18] is performed at the same theoretical level using the Gonzalez-Schlegel steepest descent path in the mass-weighted Cartesian coordinates with a step size of 0.01($amu^{1/2}$ -Bohr). Additional proof that the transition state truly connects the intended reactant and product along the corresponding potential energy surface is given by the results of IRC calculations, which are shown in Fig. 2. Table 3 summarizes the energy of each optimized geometry obtained during present study, at M06-2X/6-311++G(d,p), level of theory. In order to compute zero-point energy (ZPE) for stationary points, we have performed frequency calculation at the M06-2X/6-311++G(d,p) level of theory. Zero-point energy (ZPE) thus obtained were corrected with a scale factor of 0.967 [19] and the total energies of each species were calculated on potential energy surface. Fig. 3 shows a schematic potential energy profile of HFE-7100 reactivity with the HO_2 and NH_2 radicals using zero-point energy (ZPE) corrections. The ground state energy of HFE-7100 + HO_2/NH_2, which includes ZPE, is plotted against these energies, with zero being used randomly. For TS1 and TS2 the energy barrier determined at the M06-2X/6-311++G(d,p) level is 19.41 and 9.18 kcal mol^{1}, respectively. From these results, it can be emphasize that the hydrogen abstraction by NH_2 radical is more facile than the hydrogen abstraction by HO_2 radical.

3.1. *Kinetics calculation*

The conventional transition state theory (CTST) [20] and Eckart's tunneling correction [21] were used to calculate the rate coefficient values for various reaction channels spanning the 250–450 K temperature range using the following formula.

$$k=(T)\frac{k_B T}{h}\frac{Q^{\ddagger}_{TS}}{Q_R}\exp\frac{-\Delta E}{RT}(3)$$

The represents symmetry factor whereas tunneling correction factor at temperature T is represented by the symbol (T). The total partition functions (per unit volume) for the reactants and transition states are denoted by Q_R and ,, respectively. R stands for the universal gas constant, k_B for the Boltzmann constant, h for Planck's constant, and E for the barrier height incorporating zero point energy correction. The value of symmetry factor for reaction channels (12) has been taken as 3. The obtained rate coefficients in the temperature range of 250 – 450 K for reaction pathways (1–2) are recorded in Table 4. At 298 K, our calculated rate constant for TS1 and TS2 were found to be 4.09×10^{29} and 1.79×10^{18} cm^3 $molecule^{1}$ s^{1} respectively at M06-2X/6-311++G(d,p) level of theory. The results in this study are very important to understand the mechanism and kinetics

of the atmospheric reactions of HFE-7100 with other species such as NH_2, CH_3, etc. They will help researchers in working with various experiments related to this species in the future.

4. Conclusions

The mechanism and kinetics, as well as thermodynamics of the atmospheric reaction of HFE-7100 with HO_2 & NH_2 radicals have been investigated based on the quantum chemical theory. The DFT method in conjunction with the basic set 6-311++G(d,p) has been employed to optimize for the species related in this reaction, such as reactants, intermediate states, transition states, and products. Single-point energies for all species on the potential energy surface has been calculated using M06-2X/6-311++G(d,p) level. The reaction channel follows an indirect path through the formation of pre- and post- reaction complexes on the potential energy surface. The thermal rate constant for the H atom abstraction of HFE-7100 by HO_2 and NH_2 radical is found to be 4.09×10^{29} and 1.79×10^{18} cm^3 $molecule^1$ s^1 at 298 K. Our results suggest that hydrogen abstraction by NH_2 radical is likely the dominant route for the atmospheric oxidation of HFE-7100 under reaction conditions.

Acknowledgments: BKM acknowledges financial support from the Department of Science and Technology, New Delhi in the form of project under DST-SERB CRG scheme (CRG/2023/002561).

Conflict of Interest- The Authors declare no conflict of interest.

Data Availability- Data sharing is not applicable to this article.

Funding Declaration- The research presented in the article does not receive external funding from grants, agencies, or organizations.

AI Usage Declaration- No generative AI tools were used in the preparation of this manuscript.

Author's Contribution- Conceptualization: NP & NKG; Methodology, BKM and DD;

Writing, review & editing, all authors. All authors have read and agreed to the published version of the manuscript.

References

[1] R. L Powell, **"**CFC phase-out: have we met the challenge", *J. Fluorine Chem*., Vol. 114, No. 2, pp. 237-250, April 2002. /doi.org/10.1016/S0022-1139(02)00030-1

[2] A. Sekiya and S. Misaki, **"**The potential of hydrofluoroethers to replace CFCs, HCFCs and PFCs", *J. Fluorine Chem*., Vol. 101, No. 2, pp. 215-221, Feb 2000, https://doi.org/10.1016/S0022-1139(99)00162-1

[3] M. Misale, G. Guglielmini and A. Priarone, "HFE-7100 pool boiling heat transfer and critical heat flux in inclined narrow spaces", *Int. J. Refrig*., Vol. 32, No. 2, pp.235-245, March 2009, DOI: 10.1016/j.ijrefrig.2008.06.003

[4] A. A. Zakhidov, J. K Lee, H. H. Fong, J. A. DeFranco, M. Chatzichristidi, P. G. Taylor, C. K. Ober and G. G. Malliaras, "Hydrofluoroethers as Orthogonal Solvents for the Chemical Processing of Organic Electronic Materials", *Adv. Mater*., Vol. 20, No. 18, pp. 3481–3484, Sept 2008, **https://doi.org/10.1002/adma.200800557**

[5] T. J. Wallington, W. F. Schneider, J. Sehested, M. Bilde, J. Platz, O. J. Nielsen, L. K. Christensen, M. J. Molina, L. T. Molina and P. W. Wooldridge, "Atmospheric Chemistry of HFE-7100 (C4F9OCH3): Reaction with OH Radicals, UV Spectra and Kinetic Data for C4F9OCH2· and C4F9OCH2O2· Radicals, and the Atmospheric Fate of C4F9OCH2O· Radicals", *J. Phys. Chem. A*, Vol. 101, No. 44, pp. 8264-8274. Oct. 1997, https://doi.org/10.1021/jp971353w

[6] F. Cavalli, M. Glasius, J. Hjorth and B. Rindone, "Atmospheric lifetimes, infrared spectra and degradation products of a series of hydrofluoroethers", *Atmos. Environ*., Vol. 32, No. 1, 3767–3773. Nov 1998, https://doi.org/10.1016/S1352-2310(98)00106-X

[7] I. Bravo, Y. Dıaz-de-Mera, A. Aranda, K. Smith, K. P. Shine and G. Marstond, "Atmospheric chemistry of $C_4F_9OC_2H_5$ (HFE-7200), $C_4F_9OCH_3$ (HFE-7100), $C_3F_7OCH_3$ (HFE-7000) and $C_3F_7CH_2OH$: temperature dependence of

the kinetics of their reactions with OH radicals, atmospheric lifetimes and global warming potentials", *Phys. Chem. Chem. Phys.*, Vol. 12, No. 19, 5115–5125, May 2010, https://doi.org/10.1039/b923092k

[8] A. Aranda, Y. Diaz-De-Mera, I. Bravo, D. Rodriguez, A. Rodroguez and E. Martinez, "Atmospheric HFEs Degradation in the Gas Phase: Reactions of HFE-7100 and HFE-7200 with Cl Atoms at Low Temperatures", *Environ. Sci. Technol.*, Vol. 40, No. 19, 5971-5976, Aug 2006, https://doi.org/10.1021/es060495d

[9] B. K. Mishra, M. Lily, R. C. Deka and A. K. Chandra, "A theoretical insight into atmospheric chemistry of HFE-7100 and perfluoro-butyl formate: reactions with OH radicals and Cl atoms and the fate of alkoxy radicals", *New J. Chem*, Vol. 40, No. 7, pp. 6148-6155, July 2016, https://doi.org/10.1039/c5nj02752g

[10] M. J. Frisch. et al. Gaussian 09, Revision B.01; Gaussian, Inc.: Wallingford, CT. 2010.

[11] Y. Zhao and D. G. Truhlar "The M06 Suite of Density Functionals for Main Group Thermochemistry, Thermochemical Kinetics, Noncovalent Interactions, Excited States and Transition Elements: Two New Functionals and Systematic Testing of Four M06-Class Functionals and 12 Other Functionals. *Theor. Chem. Acc.*, Vol. 120, pp. 215-241, May 2008, https://doi.org/10.1007/s00214-007-0310-x

[12] N. K. Gour, K. Borthakur, S. Paul and R. C. Deka, "Tropospheric degradation of 2-fluoropropene (CH_3CFCH_2) initiated by hydroxyl radical: Reaction mechanisms, kinetics and atmospheric implications from DFT study", *Chemosphere*, Vol. 238, pp.124556, Jan. 2020, https://doi.org/10.1016/j.chemosphere.2019.124556

[13] N. Tayum, N. K. Gour, A. Murugan and B. K. Mishra, "Theoretical Insights into the Reactivity of M2CAA with OH Radicals and the Fate of Resulting Alkoxy Intermediates", *ChemistrySelect*, Vol. 11, No. 1, pp. e04798, Jan. 2026, https://doi.org/10.1002/slct.202504798

[14] P. Gogoi, S. Paul, B. K. Mishra, N. K. Gour and R. C. Deka, "Tropospheric Oxidation of 1H-Heptafluorocyclopentene (cyc-CF2CF2CF2CF=CH−) with OH Radicals: Reaction Mechanism, Kinetics, and Global Warming Potentials", *ACS Earth Space Chem*. Vol. 5, No. 7, pp.1792−1800, July 2021, https://doi.org/10.1021/acsearthspacechem.1c00124

[15] N. Tayum, A. Murugan, R. C. Deka, N. K. Gour, and B. K. Mishra, "The molecular level study of the fate of the $CH_3CH_2C(O)OCH(O)CH_3$ radical derived from ethyl propionate", Molecular Simulation, Vol. 49, No. 7, pp. 711-719, Mar. 2023, https://doi.org/10.1080/08927022.2023.2189975

[16] S. Paul, B. K. Mishra. S. D. Baruah, R. C. Deka and N. K. Gour, "Atmospheric oxidation of HFE-7300 [n-$C_2F_5CF(OCH_3)CF(CF_3)_2$] initiated by •OH/Cl oxidants and subsequent degradation of its product radical: a DFT approach", *Env. Sci. Poll. Res.*, Vol. 27, No. 1, pp. 907-920, Jan. 2020, https://doi.org/10.1007/s11356-019-06975-1

[17] N. K. Gour, B. K. Mishra, P. J. Sarma, P. Begum and R. C. Deka, "Tropospheric degradation of HFE-7500[n-$C_3F_7CF(OCH_2CH_3)CF(CF_3)_2$]initiated by Cl radicals and Fate of alkoxy radical [n-$C_3F_7CF(OCH(O)CH_3)CF(CF_3)_2$]: A DFT investigation", *J. Fluor. Chem.*, Vol. 204, pp.11−17, Dec. 2017, https://doi.org/10.1016/j.jfluchem.2017.09.010

[18] C. Gonzalez and H. B. Schlegel, "An improved algorithm for reaction path following: higher− order implicit algorithms", *J. Chem. Phys.*, Vol. 95, No. 8, pp.5853−5860, Oct. 1991, https://doi.org/10.1063/1.461606

[19] I. M. Alecu, J. Zheng, Y. Zhao and D. G. Truhlar, "Computational Thermochemistry: Scale Factor Databases and Scale Factors for Vibrational Frequencies Obtained from Electronic Model Chemistries", *J. Chem. Theory Comput.*, Vol. 6, No. 9, pp. 2872-2887, Aug. 2010, https://doi.org/10.1021/ct100326h

[20] K. J. Laidler. Chemical Kinetics, 3rd edn. New Delhi, Pearson Education, 2004.

[21] R. Xiao, M. Noerpel, H. L. Luk, Z. Wei and R. Spinney. "Thermodynamic and kinetic study of ibuprofen with hydroxyl radical: A density functional theory approach", *Int. J. Quant. Chem.*, Vol 114, No. 1, pp. 74-83. Jan. 2014, **https://doi.org/10.1002/qua.24518**

Table1 Thermochemical data for reaction channels (12) calculated at M06-2X/6-311++G(d,p) level of theory. All values are in kcal mol^{-1}.

Reaction channels	$\Delta_r H°$	$\Delta_r G°$
Reaction 1	15.16	14.73
Reaction 2	-6.00	-6.02

Table 2 Harmonic vibrational frequencies of reactants, transition states and products at M06-2X/6-311++G(d,p) level of theory.

Species	Vibrational Frequencies (cm-1)
HFE-7100	45, 55, 68, 75, 113, 159, 167, 216, 224, 245, 251, 295, 330, 338, 341, 366, 392, 428, 516, 543, 557, 597, 611, 632, 707, 754, 802, 895, 1058, 1143, 1170, 1189, 1190, 1206, 1242, 1257, 1275, 1285, 1297, 1349, 1373, 1435, 1495, 1508, 1516, 3078, 3164, 3197
TS1	1792i, 34, 43, 62, 78, 87, 109, 133, 136, 169, 215, 230, 242, 249, 282, 294, 331, 341, 352, 368, 391, 403, 441, 510, 522, 542, 558, 597, 605, 610, 634, 707, 754, 801, 899, 1083, 1102, 1112, 1158, 1187, 1191, 1204, 1208, 1240, 1268, 1274, 1295, 1298, 1353, 1363, 1433, 1441, 1481, 1559, 3121, 3239, 3801
TS2	1849i, 28, 45, 53, 68, 98, 116, 149, 155, 172, 216, 226, 249, 254, 297, 330, 337, 341, 366, 368, 394, 431, 515, 542, 556, 579, 600, 611, 634, 707, 751, 780, 798, 835, 903, 1072, 1136, 1150, 1174, 1191, 1211, 1243, 1260, 1274, 1292, 1298, 1348, 1371, 1413, 1434, 1469, 1489, 1559, 3117, 3223, 3428, 3525
RC1	26, 41, 53, 63, 69, 80, 112, 148, 160, 170, 200, 213, 221, 237, 250, 264, 296, 330, 339, 348, 368, 392, 430, 472, 519, 543, 561, 599, 613, 632, 708, 754, 806, 892, 1042, 1146, 1190, 1191, 1197, 1207, 1238, 1256, 1274, 1280, 1283, 1296, 1352, 1364, 1432, 1488, 1504, 1507, 1517, 3097, 3189, 3225, 3616
RC2	33, 38, 68, 69, 72, 106, 132, 155, 168, 171, 199, 222, 228, 249, 251, 295, 300, 330, 337, 344, 366, 3963, 413, 430, 517, 542, 556, 597, 609, 633, 706, 754, 801, 893, 1049, 1141, 1164, 1188, 1190, 1204, 1236, 1257,1273, 1289, 1297, 1349, 1373, 1434, 1491, 1503, 1514, 1540, 3075, 3169, 3194, 3412, 3505,
PC1	31, 45, 65, 72, 79, 94, 112, 117, 134, 143, 172, 210, 221, 231, 249, 255, 285, 295, 332, 342, 355, 369, 394, 429, 502, 523, 544, 558, 576, 605, 612, 633, 707, 756, 801, 901, 1035, 1105, 1159, 1185, 1193, 1201, 1239, 1250, 1277, 1278, 1297, 1353, 1365, 1381, 1432, 1476, 1479, 3190, 3353, 3821, 3840
PC2	19, 39, 45, 63, 70, 101, 112, 125, 144, 177, 195, 216, 233, 248, 255, 269, 294, 321, 332, 340, 351, 368, 394, 430, 515, 543, 550, 595, 611, 631, 638, 707, 755, 802, 903, 1073, 1102, 1171, 1188, 1194, 1199, 1240, 1260, 1272, 1289, 1297, 1352, 1368, 1432, 1469, 1665, 1669, 3195, 3359, 3510, 3634, 3642
H2O2	417, 1037, 1344, 1499, 3859, 3861
HO2	1257, 1460, 3708
CF3CF2CF2C F2OCH2 (P)	44, 56, 69, 103, 115, 167, 204, 218, 224, 244, 251, 295, 331, 338, 349, 366, 393, 429, 515, 543, 556, 584, 603, 611, 633, 707, 755, 800, 901, 1110, 1169, 1185, 1193, 1201, 1245, 1259, 1277, 1286, 1299, 1350, 1370, 1435, 1481, 3181, 3334
NH2	1503, 3404, 3499
NH3	1029, 1671, 1672, 3526, 3660, 3661

Table 3 Relative energies (in kcal mol^{1}) with zero-point energy correction for the reactants, reaction complexes, transition states, product complexes and products at M06-2X/6-311++G(d,p) level of theory.

Species	M06-2X/6-311++G(d,p)
HFE-7100 + HO_2/NH_2	0
RC1	-6.27
RC2	-3.67
TS1	19.41
TS2	9.18
PC1	10.66
PC2	-9.04
P + H_2O_2	15.00
P + NH_3	-6.03

Table 4: Rate constants of different reaction channels and overall rate constant (in cm^3 $molecule^1$ s^1) within the temperature range of 250450 K at M06-2X/6-311++G(d,p) level of theory.

Rate constant	250 K	298.15 K	300 K	350 K	400 K	450 K
k_1	9.13×10^{-32}	4.09×10^{-29}	4.98×10^{-29}	4.08×10^{-27}	1.55×10^{-25}	2.35×10^{-24}
k_2	9.81×10^{-19}	1.79×10^{-18}	1.83×10^{-18}	4.50×10^{-18}	1.14×10^{-17}	2.69×10^{-17}

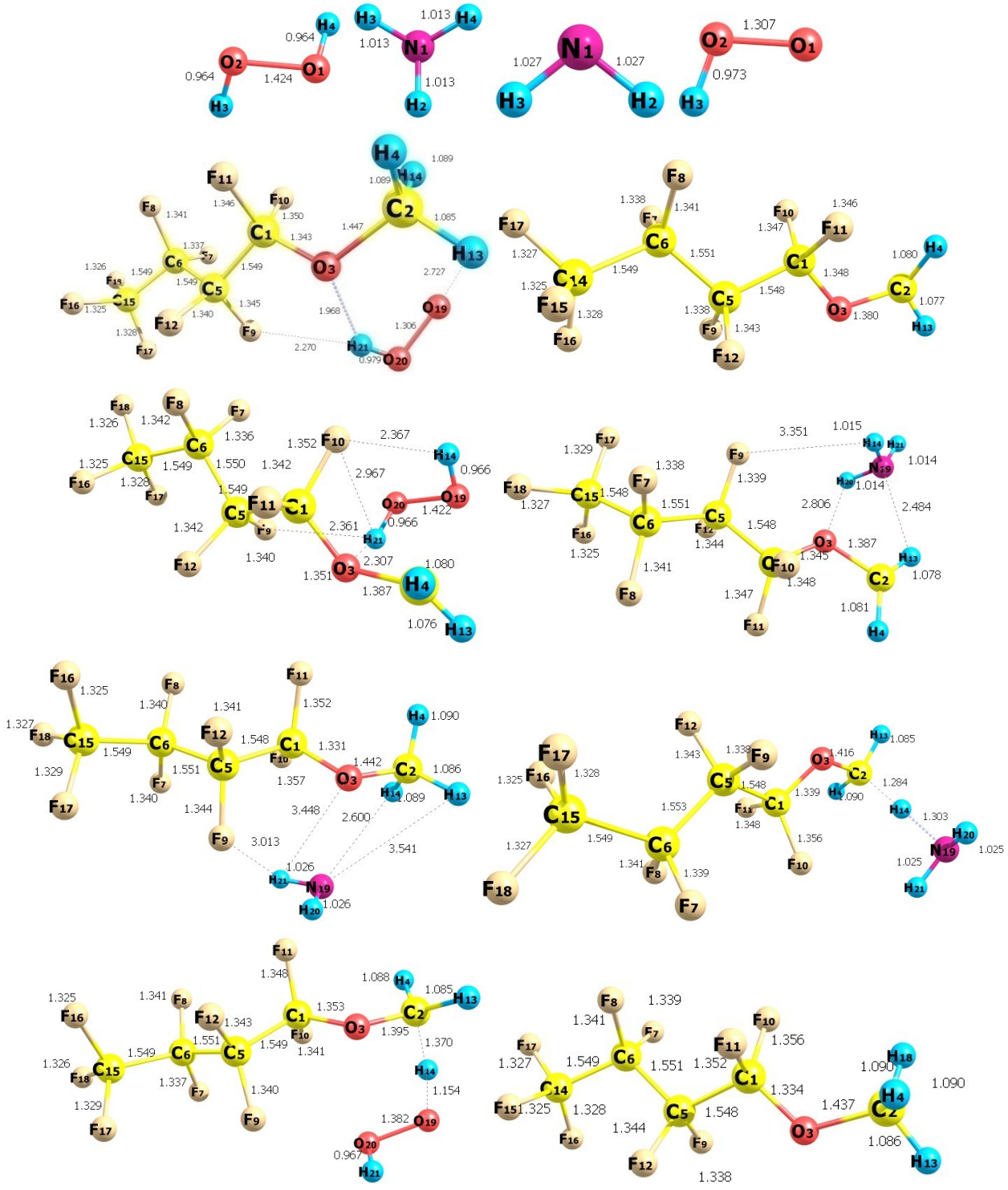

Fig. 1: Optimized geometry of reactants, reaction complexes, transition states, product complexes and products obtained at M06-2X/6-311++G(d,p) level of theory. Bond lengths are in angstroms.

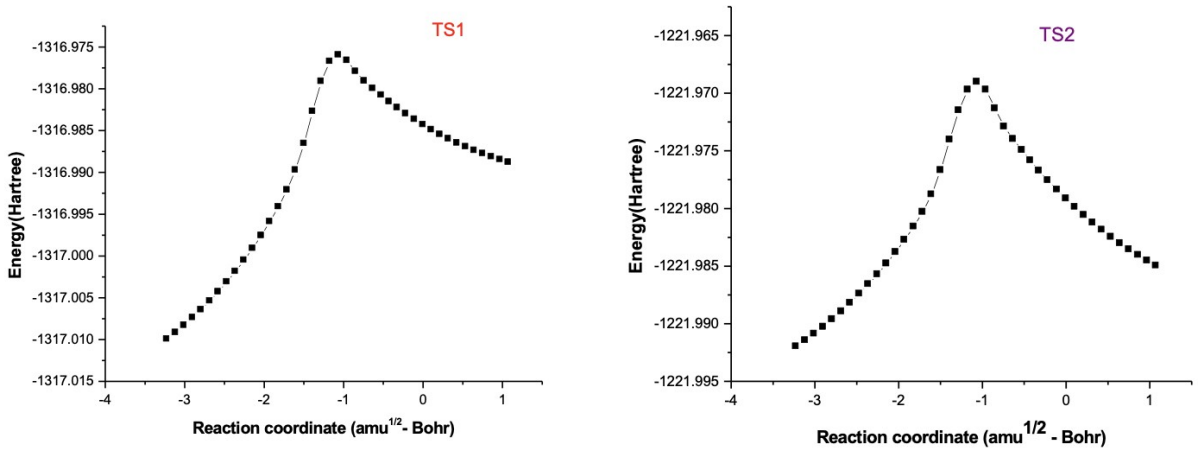

Fig. 2: IRC plots performed for transition states TS1 and TS2 obtained at M06-2X/6-31!++G(d,p) level of theory.

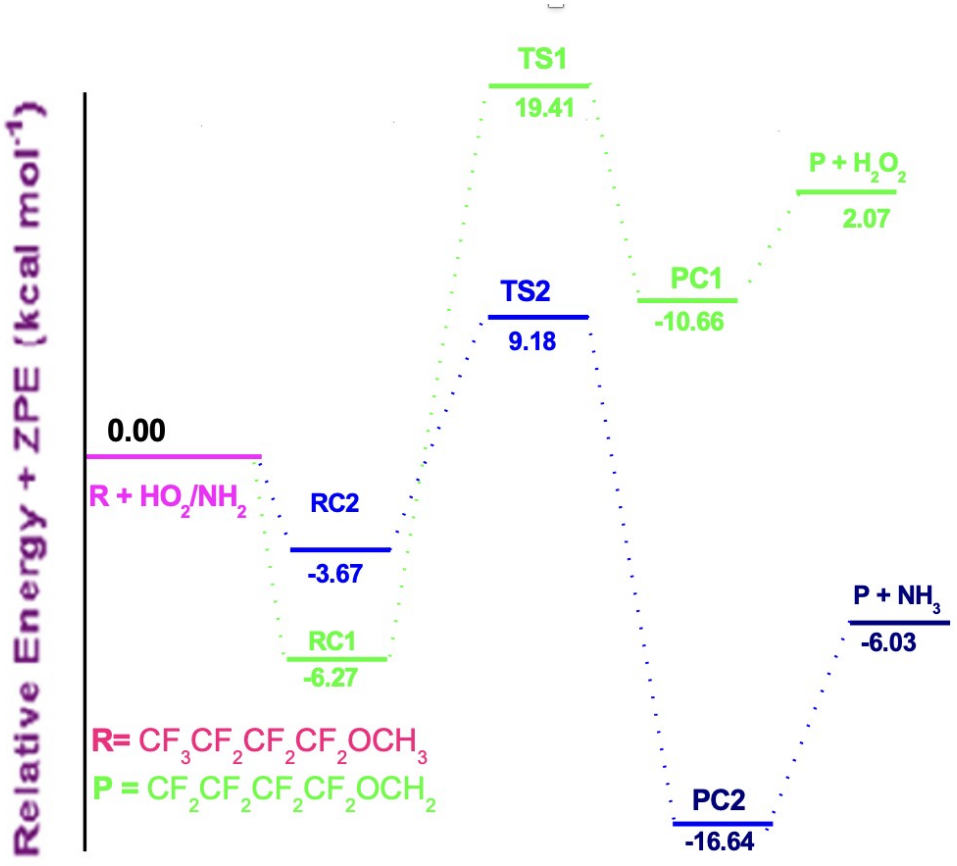

Fig. 3: Potential energy diagram for the reaction of HFE-7100 with HO_2 and NH_2 radicals at M06-2X/6-311++G(d,p) level of theory.